

## Chapter

# Optically Clear Adhesives for OLED

*Joel T. Abrahamson, Hollis Z. Beagi, Fay Salmon  
and Christopher J. Campbell*

## Abstract

Optically clear adhesives (OCA) have been used for more than a decade to bond rigid LCD and AMOLED displays for consumer electronics applications, offering optical, mechanical, and electrical performance benefits. The performance requirements of an OCA to bond cover window, touch sensors, and circular polarizers in a plastic OLED display to bent cover glass or a flexible, foldable OLED display are drastically different from a flat, rigid device. For plastic OLED to bent cover glass bonding, the adhesive needs to be strong enough to resist spring back of the flat, plastic OLED devices. For flexible, foldable OLED displays, the neutral plane needs to be managed during folding keeping strain to a minimum in critical layers of the device (e.g., touch sensor, TFT, TFE), and the OCA cannot deform (or cause other layers to deform) during the folding process. Folding also brings challenges to touch sensors that can no longer use conventional passivation layers. As a result, the OCA will be responsible for preventing corrosion of touch sensor materials such as metal mesh, silver nanowire, carbon nanotube, and graphene. The chapter will discuss OCA performance requirements for rigid, flexible, and foldable OLED bonding.

**Keywords:** adhesives, OLED, optically clear, OCA, LOCA, displays, bonding, consumer electronics

## 1. Introduction

Optically clear adhesives (OCA) and liquid optically clear adhesives (LOCA or OCR for optically clear resins) have been used in consumer electronics, industrial and automotive bonding solutions for more than 15 years. OCA usage increased significantly as consumer electronics devices saw the transition from resistive to capacitive touch with its first implementation in the LG Prada phone in 2006 [1]. The advantage of using an OCA shows improvements in mechanical, optical and electrical performance of the display module and device. The initial application in OCAs in rigid OLED-based devices was similar to LCD devices, but as plastic OLED (pOLED) devices were introduced to the market, OCAs enabled new form factors, such as curved OLEDs in the Galaxy Round and Galaxy Gear S [2] as well as the Galaxy Note Edge [3].

There are two important mechanical considerations for optically clear adhesives – does it stick (adhesive strength) and how strong is it (cohesive strength). Adhesive strength can be defined by the work of adhesion, which is the amount of work required to separate the adhesion from the adherend. Adhesion can be achieved

through van der Waals interactions, hydrogen bonding, acid–base, ionic, covalent and mechanical interlocking [4–6]. Film based OCAs are pressure sensitive adhesives, while LOCAs are liquids that are dispensed and cured. Pressure sensitive adhesives exhibit tack when the modulus is below  $3 \times 10^5$  Pa or the so-called Dahlquist criterion [7] at the application temperature.

Once the adhesive sticks, the cohesive strength of the material determines the mechanical properties of the bond. Conventional adhesives are functional to the point of bond failure. For optically clear adhesives, they are functional to the point of cavitation that can occur at a significantly lower strength than bond failure [8]. The cohesive strength of an OCA can be designed to resist cavitation and bubble formation when it is warranted.

OCAs are often tested for reliability and durability at elevated temperatures and humidity (e.g. 65°C/90% RH). It is important to have sufficient adhesive strength to maintain performance through these conditions. Potential failure modes include moisture ingress at the interface and bulk plasticization of the adhesive. The adhesive should be selected to have sufficient strength based on the design of the module/device and the necessary durability for the adhesive.

Optically clear adhesives are typically based on acrylate chemistry, having a refractive index of 1.47–1.48 that is comparable to glass and other important materials (e.g. PET, polarizer, etc.) in a display device. By matching the index and using an adhesive to replace an air gap, this significantly reduces the amount of light reflected at an interface ( $\sim 4\%$  [9]). By using an OCA, both contrast and brightness can be improved in a device.

Reliability and durability of OCAs in elevated temperatures and humidity can have an impact on optical properties. The adhesive can absorb moisture under these conditions, becoming supersaturated at elevated temperatures. When the adhesive returns to ambient conditions, the excess moisture phase separates in the material becoming apparent as haze in the bulk of the material. This can be avoided by designing the adhesive to be anti-whitening [10]. Durability under UV exposure is a requirement in automotive and high performing consumer electronics applications. A common failure mode under these conditions is yellowing. Careful materials selection and formulation by the materials supplier can prevent yellowing by UV. Circular polarizers in OLED devices can reduce UV transmission to the OLED panel [11]. As POL-less devices [12] become a reality, the OCA will need to take on UV blocking functionality to protect the OLED device.

The electrical functionality of OCAs includes protecting sensitive touch sensors as well as enabling superior touch functionality. Industrial pressure sensitive adhesives often contain acrylic acid [13] to achieve good adhesion. Acidic species corrode touch sensors, such as ITO. Therefore, adhesives selected for bonding in optical applications must be acid-free. The potential module stack configurations for touch will be described in the next section. OCAs can be designed with an optimal dielectric constant at the touch sensing frequency (100 kHz) [14] from low ( $D_k < 3$ ) to high ( $D_k > 9$ ) to maximize the signal-to-noise ratio and minimize current and power to drive the touch circuit.

## **2. Key requirements and challenges in OLED optical bonding**

The first OLED displays bonded in consumer electronics were rigid (**Figure 1a**) and sealed in glass barriers. While they cannot provide the promise of flexible form factors, the OLED patterning process can still make non-rectangular form factors such as rounded corners or notches, although LCDs can now also create these shapes of viewing areas. Rigid OLEDs also can provide higher contrast and wider

color gamut compared to liquid crystal displays (LCDs), but the requirements for the adhesive are not dissimilar to those for rigid LCD optical bonding.

When OLEDs are manufactured on thin, plastic substrates like polyimide, they can enable new form factors that are bent or formed into curved shapes (**Figure 1b–d**). Now many different manufacturers are introducing dynamically flexible devices that can fold repeatedly, such as the Royole FlexPai [15], Samsung Galaxy Fold [16], and Huawei Mate X [17]. Besides these single-axis folding devices, the LG Signature OLED TV R9, announced in 2019 [18], demonstrates that even very large OLED modules can be constructed to roll open and closed from a cylindrical shape less than 30 cm in diameter. Although TVs are not often touch-enabled, this type of flexible device should still use optical bonding to add protective layers to the OLED.

Whatever the form factor, OLED display modules all require additional layers for durability, user interface, and optical functionality. At least one layer each of cover window (CW), touch sensor (TS), and circular polarizer (CP) is generally included, and these must be laminated together with OCA or LOCA for best contrast, brightness, and mechanical durability. The cover window is generally made of glass, although in a few cases manufacturers have used plastics like polycarbonate (PC), polyethylene terephthalate (PET), or clear polyimide (CPI). Plastic cover windows will not shatter and can more easily flex to meet the needs of dynamically foldable or flexible displays. Commonly an ink border or bezel, 10–60  $\mu\text{m}$  thick, is printed around the perimeter of the CW to hide non-transparent supply circuitry in the TS and display layers.

The touch sensor itself may include a thin passivation layer over the functional layer (usually made of ITO, but sometimes metal mesh or silver nanowires) to protect the sensor from environmental aggressors. The CP may be positioned above the touch sensor (**Figure 1b**) to decrease the visibility of circuit patterns in the touch sensor. While **Figure 1** shows at most one separate TS layer, closely related to

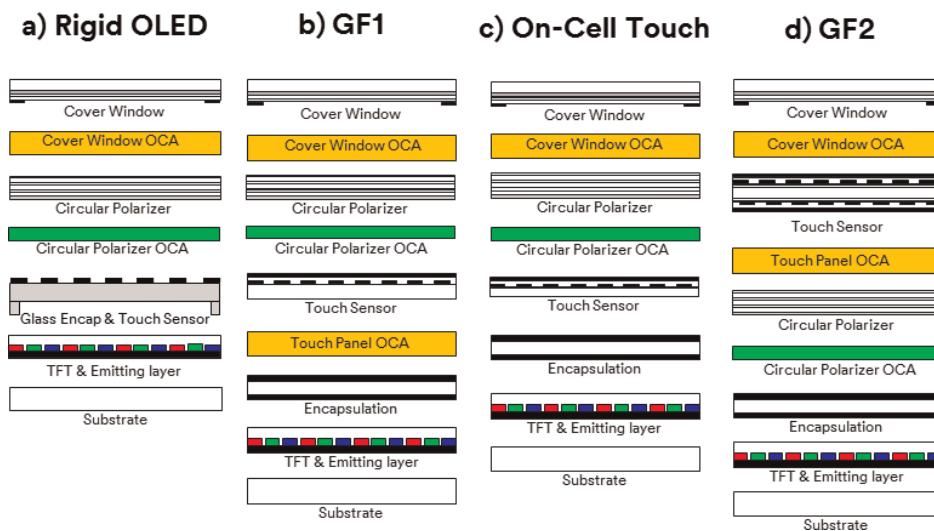


**Figure 1.** OLED displays may be categorized according to the type of encapsulation and touch sensor used. (TFT = thin film transistor) (a) Rigid OLED, so named because the OLED is protected by an inflexible glass barrier with frits sealing the edges. Such designs may use a transparent conductor deposited on the glass as a touch sensor or use a separate film layer, as in (b) and (d). Architectures b-d use thin, flexible encapsulation (TFE), enabling these OLED to flex and bend. (b) GF1 means one glass cover and one film touch sensor layer. (c) On-cell touch, also called touch on encapsulation (TOE), is similar to (a) but with the sensor deposited on the flexible encapsulation layer. Therefore, the sensor substrate can be thinner than in GF1. (d) Another popular design emphasizing touch performance is GF2, which uses a single film layer with touch sensing layers patterned on both sides. (Graphic by Erik Iverson, 3M Display Materials & Systems Division).

GF2 (**Figure 1d**) is GFF (not pictured), in which two films comprise the touch sensor, each with one sensing layer, adhered with a thin OCA between them. Without separate sensor layers to resolve horizontal and vertical position, the touch sensitivity and precision of a GF1 design may be less than a GF2 design.

## 2.1 Optically clear adhesive requirements

As of 2018, OLEDs were used almost exclusively in smartphones and smartwatches, so special requirements for bonding larger displays (*e.g.*, notebooks, monitors) are less defined at present. The requirements and benefits of optical adhesives are most defined for the Cover Window OCA (often called OCA1) and Touch Panel OCA (OCA2 or OCA3, depending on the position of the polarizer). Either of these adhesives may also be a liquid resin (OCR).

Besides the general requirements for optical adhesives described in Section 1, OCA1 requires a balance between adhesive strength and capability to cover the step height of the ink bezel. Certainly strength, usually in terms of a high shear modulus, is critical to help the whole display resist impacts, a major source of user frustration every day when screens break. OCA1 is closest to an impact event on the cover window surface, but all adhesives bonded together in the display system will contribute to its resilience to impacts when the device is dropped.

On the other hand, the OCA must move sufficiently under the shear forces of lamination but then hold its position and shape afterwards, even through temperature cycles of regular use. As bezels are often now less than 1 mm wide, the OCA must bond over an ink step that may be less than 10 times longer than it is high – a challenging aspect ratio to cover without trapping an air bubble at the base of the ink step. Furthermore, the OCA must be strong enough to resist temperature cycling and moisture exposure that could pull it away from the ink step, creating edge bubbles. Bending the display around a curved edge only increases the stress on the adhesive and magnifies the challenges.

The inherent viscoelasticity of OCAs as pressure-sensitive adhesives enables good step coverage of ink or flexible printed circuit (FPC) bond lines. However, as design trends push displays to be thinner and thinner, the solution for great step coverage often comes with UV post-curable OCAs, when narrow bezels make LOCA impractical. Such OCAs are applied in a more viscous, yet still solid, film form with some initial tack. They can flow with the pressure of lamination to cover steps ink steps that are 30–50% the thickness of the OCA. A heated autoclave process step may further improve step coverage capability. Then the laminate is irradiated with light, generally in the UVA spectrum, to increase the bonding within the adhesive, effectively “locking” it in place to improve its durability to the level of a high-modulus adhesive.

In most designs, especially those with the touch sensor on the encapsulation (**Figure 1a, c**), OCA1 benefits from a higher  $D_k$ , as much as 9, to increase capacitive coupling between the finger and the sensor. However, designs with a separate touch sensor (**Figure 1b, d**) often require a *lower*  $D_k$ ,  $< 3$ , for the touch panel OCA to decrease coupling of electromagnetic interference (EMI) noise from the display. In either case, however, stability of  $D_k$  is important, over operating temperatures and humidity (moisture absorption generally increases  $D_k$ ) and through the life of the device, as an accelerated aging test would simulate.  $\Delta D_k < 0.3$  is a good guideline, and higher performance applications may require a narrower range.

These properties benefit reliability, durability, and esthetics – all values to the end user of the device. On the other hand, manufacturers and the display supply chain have other requirements. To improve overall process yield and efficiency, these players desire re-workability: targeted or triggered failure of the



adhesive cleanly and without residue from one interface. Then components may be separated; expensive parts, especially the OLED and the cover glass, may be recovered. The challenge is that the re-work condition – be it heat, cold, light exposure, or some other factor – must be outside the realm of normal operating conditions so that the display does not de-bond prematurely after it leaves the factory line.

Dimensional stability is another property more visible to the manufacturers than to the end user. OCAs may be delivered as master rolls, and LOCAs will be dispensed or printed as a liquid, but for aggressive tolerances and more complex shapes like rounded corners, manufacturers often opt for individual pre-cut adhesive parts. In that case, the cut OCA must maintain its shape and dimension through environmental conditions of shipping and duration of expected shelf life. The flow, creep, or oozing of the adhesive at elevated temperatures must be limited; consider that the inside of an uncontrolled shipping container can easily exceed 50° C. Similarly, the shipment and packaging format interplays with the formulation; the sustained pressure of a stack of cut parts should also cause only minimal oozing. These properties for cut-part stability are often at odds to the viscosity needed for an uncured PSA to cover steps, as described earlier.

Most OCAs for display bonding are designed to resist whitening, as described in the previous section. Some degree of water resistance has been valuable in OCAs, but the next frontier may be resistance to a broader range of chemical ingress, especially for designs in which the bezels are very narrow or non-existent. Wearable displays also encounter more splashes compared to phones, which may often be partly protected inside a pocket or bag. Normally, a rim tape or lens bonding adhesive may adhere the cover window to the device housing underneath the bezel, and materials chemists may use a wider range of polymers to block chemical ingress, since the material does not need to be optically transparent. The challenge is heightened since everyday chemicals that might contact screens include oils/fats (cooking oil, sweat), alcohols, acids (soda, vinegar), and bases (ammonia, cleaning products) – both hydrophobic and hydrophilic substances.

While manufacturers generally select OCAs for OLED separately from the layers they bond, the CP OCA is widely sold with the CP itself, a different supply chain. Thus, low cost for the integrated product is key, in addition to technical requirements of good adhesion to the CP at a thickness of  $\leq 25 \mu\text{m}$ . Since the polarizer absorbs a large fraction of UV light, this OCA cannot practically be UV post-curable. As future CPs continue to decrease in thickness [19–21], with thinner protective layers around the optically active layers, the CP OCA may need to serve a greater role in protecting the polarizer from harmful environmental factors.

## **2.2 Bonding requirements in bent or curved displays**

The performance requirements of an OCA to bond layers in a flexible OLED display are quite different from a rigid, flat device. The neutral plane must be balanced to minimize strain in critical layers of the device. Thin film transistors (TFTs), thin flexible encapsulation (TFE), and touch sensors are predicted to be most vulnerable, although newer silver nanowire and metal mesh sensors are more flexible than ITO [22, 23]. Although manufacturers continue to improve the durability of OLED displays, publicly available literature indicates that critical components are still quite sensitive to strain. The SiO<sub>2</sub> layer of the TFT on polyimide may break at 0.2% tensile strain [24] and the TFE at around 0.3% in bending [25].

When the form of the device requires the OLED to bend only once (during manufacturing), the cover window can be made of glass, which offers the best

resistance to scratches and protects the display from impacts to the screen. However, the modulus (*i.e.*, stiffness) of the glass is much higher than the other plastic films of the display (polarizer, touch sensor, OLED), whereas the plastic films feel a “spring-back” force due to their tendency to relax back to their original flat form. Since the glass will not move or deform, the OCAs in the curved display module must have very high adhesion to hold the plastic films in their curved state; otherwise they will pull away from the glass at the bend and leave bubbles.

Examples of OCAs that have the strength needed for durable curved bonding are 3M™ Contrast Enhancement Films (CEF) 30xx and 31xx, where xx denotes the thickness in mils. **Table 1** describes one important property, peel adhesion, for these adhesives. Their primary difference is that CEF30xx is UV post-curable for step coverage, as described above, and its samples in the table were cured with  $1 \text{ J/cm}^2$  UVA prior to peel testing.

### 2.3 Bonding requirements in dynamically flexible displays

To minimize strain on a flexible OLED display, an adhesive should either perfectly mechanically decouple the layers from each other in bending (*i.e.*, with very low modulus) or adjust the position(s) of the neutral plane(s) during the bend. Plastic OLED displays have some inherent flexibility and have been demonstrated to fold thousands of times to a radius of 4 mm or less [26, 27], but the right adhesives are required to integrate the display layer into a durable, functional device while maintaining that flexibility. Besides balancing the neutral plane(s) to minimize strain on the OLED, when the device is folded closed, the adhesive should have minimal creep to avoid flowing and changing in thickness in response to stress. Upon unfolding the device, no buckles or wrinkles should be visible, and the adhesive should assist it in recovering quickly to a flat, smooth profile. Finally, all these adhesive properties should vary as little as possible over the operating temperatures and conditions of the device. These requirements point to a soft, elastic material with a low glass transition temperature ( $T_g$ ), below the minimum operating temperature. If operating temperatures often extend down to  $-20^\circ\text{C}$ ,  $T_g < -30^\circ\text{C}$  would be a minimal requirement.

The elasticity requirement contrasts with the common viscoelasticity of OCAs in static applications, and a soft (low modulus) adhesive would typically also sacrifice adhesion. Practically speaking, the foldable OCA should still maintain peel adhesion of  $1 \text{ N/cm}$  at a minimum. The surface energy and cleanliness of the interfaces with the adhesive also affect adhesion, however, so this property may be improved with plasma treatment or primer layers to increase surface energy.

When a flexible display is expected to bend thousands of times, a foldable OCA should retain these mechanical properties with minimal shift or hysteresis through repeated stress/strain cycling. Besides testing in application, the adhesive properties may be characterized through tensile, compressive, and shear loading, for example,

OCA Name	Thickness ( $\mu\text{m}$ )	20 min dwell	3 d dwell
CEF3004	100	11.2	14.0
CEF3006	150	15.1	17.4
CEF3104	100	11.0	14.1
CEF3106	150	12.0	15.2

*ASTM D3330 modified test method, 1-cm-wide strips, 305 mm/min peel rate, 2.0 mil polyester backing. All dwells at  $23^\circ\text{C}/50\%$  relative humidity.*

**Table 1.**  $180^\circ$  Peel adhesion (N/cm) from float glass for curved OLED display OCAs after varying dwell times.

using mechanical load frames, rheometers, or texture analyzers [28]. Some mechanical testing to support the simulation of flexible adhesives is described later in Section 4.

Even a folding radius of 5 mm can require shear strain of >300% in the adhesives during folding (depending on the thickness of the various display layers). Foldable adhesives must certainly shear to this extent without breaking or permanently deforming but are also expected to release strain quickly when stress is removed upon unfolding. However, recovery time of the flexible display also greatly depends on the properties of the other film layers, which have much higher moduli, so it is difficult to distill the recovery requirement for the system into a generic recommendation for the adhesives.

## **2.4 Future requirements for optically clear adhesives for OLEDs**

Many trends in OLED design focus on enabling greater flexibility, and new adhesives will be needed to support this as well. Through the next decade, manufacturers will push for narrower folding/rolling radii, multiple folding axes in displays, and longer device lifetimes, especially in terms of cycles of flexing. As folding radius decreases below 3 mm, the required shear strain will likely increase from 300% to roughly 500 to 700% or more. Additional folding axes will also increase the total magnitude of shear displacement, as each axis adds its own displacement to the system. A rollable display can be considered as the limit of many axes of folding across the length of the device. Rolling devices will initially launch with radii of several centimeters, which is larger than today's one-axis folding displays, but the shear will add with each bend such that the "creep" with applied stress will be a more critical property. With larger creep, even a flexible adhesive could shear out several mm at the edge when the display is rolled, resulting in unsightly uneven edges or, worse, display layers pressing into the bezel/frame bonding and generating further stress.

Thinner display modules will assist flexibility, so trends in integrating functional components are likely to continue. These may include coated circular polarizers [19–21] or color filters integrated with the OLED encapsulation [12]. With thin flexible cover windows, expect adhesives on either side of the OLED display to play a greater role in protecting the module from impact damage. This will be especially true for plastic CWs compared to glass, since they have lower elastic moduli.

Plastic cover windows may see further growth in automotive displays, but for different reasons. Some manufacturers and safety authorities have been concerned about the possibility of display cover glass shattering in an impact or crash and thus have preferred plastic CW for safety reasons. High-performance plastic CWs are often made of PC or PMMA (poly[methylmethacrylate]), so durable bonding to these low surface energy plastics, with their tendency to release gases under heating, will be important to future automotive OCAs. The reliability and accelerated aging tests for transportation applications are generally more severe than those for consumer electronics. The displays must withstand extremes of heat (often  $-40$  to  $+110^{\circ}\text{C}$ ), humidity, and light (especially UV) irradiation, but also conditions like sand for desert environments and salt spray on the coasts. Finally, the interiors of many concept cars already feature large displays on the complex curves that designers favor for esthetics and ergonomics. Expect curved displays to grow in size and in popularity in production models in the coming years.

Although it takes time to decrease costs and prove reliability, gradually OLEDs will expand into outdoor applications as well, as consumers begin to expect a certain level of display quality from their everyday interactions with personal and mobile devices. These outdoor bonding applications will demand reliability from the OCA,

like the automotive market. Transparent OLED displays are still in their infancy and will likely require lower levels of optical absorptivity, haze, reflectivity, and color for all layers, including optical adhesives.

A different design trend in OLED displays that has already begun in today's devices is the integration or hiding of the many cameras and sensors that now support the devices' interactions with their users and environments. The goal is always to expand the active area to occupy an ever-greater fraction of the viewable front of the device. Additionally, a camera behind the display provides a more natural interaction in video calling; the camera may track a user's gaze at the same location where the user views the other person's face, giving the impression of eye contact. The implication for bonding with OCAs is stricter dimensional control and tolerance requirements, extending to non-rectangular shapes. Already many sensors and cameras can fit in a droplet or notch shape cut out of the display and adhesives at one edge of the screen. When the camera(s) are behind the display, some adhesive layers must precisely maintain a small hole in the middle of the part, as an aperture for the camera.

### **3. Folding test method development and differentiation of multi-layer concepts**

3M has been investigating fatigue and shear performance of polymer film substrates and multi-layer stacks consisting of OCAs (Optically Clear Adhesives) and polymer films in response to dynamic bending. This work was prompted, in-part, to support materials and systems development in the realm of foldable OLED (Organic Light Emitting Diode) market technologies and applications. One device that is used to study the dynamic bending performance of these films and film stacks is an internally-designed and built bend tester. Samples can be mounted to the bend tester and folded to a specific bend radius and number of bend cycles at a defined cycle rate (bend cycles per minute). From a materials perspective, failure in the form of yielding, breakage and buckling can occur during testing. In actual flexible device constructions, the light emitting and barrier layers can be compromised over certain stress and strain thresholds. These failures are influenced largely by the stress or strain amplitude as the samples are placed in the folded conformation of interest. In this section, we will discuss the methodology behind development of a controlled and repeatable folding test that minimizes bending stress on foldable test specimens, types of defects observed in single and multi-layer polymeric stacks consisting of OCA, and additional methods of concept differentiation by incorporating ITO (Indium Tin Oxide) coated PET (polyethylene terephthalate) into the multi-layer test specimens.

#### **3.1 Investigation and definition of test method parameters**

##### *3.1.1 Hinge or pivot design*

One of the first design parameters considered during initial folding test method development is the hinge design (or pivot locations) of the test apparatus. It is important to have at least some understanding of the impact of hinge design selection. Some types of hinge design can impart added strain (or stretching) on samples during the process of folding. With single hinge folding design, or folding with only one pivot point, there will be one or more critical angles in which the test specimen is stretched beyond its original length. This type of tester design is undesirable because the design of the tester can damage the samples, and will introduce



added variables, such as test specimen attachment location and attachment adhesive properties, that will dictate how much overall strain is imparted to the sample during the action of folding and unfolding. Slight changes in attachment location and attachment adhesive properties will have an impact on variability and reproducibility of the test results. Note, this logic can be applied to certain mandrel bend folding designs as well, if the strain on test specimens is not actuated to prevent sample lengthening or stretching during folding. For this reason, we have defined a dual pivot testing apparatus (**Figure 2**), which can prevent added strain or stretching of the samples during folding.

### 3.1.2 Attachment method and location

In many cases, test specimens will consist of alternating layers of polymer film and adhesive. The primary roles of the adhesive in such constructions will be to adhere the layers together and to prevent added strain on sensitive layers, such as the display or fragile coatings. The mechanical benefit of the adhesive is maximized when specimen layers can freely move and shear across one another during folding and unfolding, thus minimizing stress on fragile layers. For this reason, attaching specimens to the test apparatus using adhesive (instead of clamping) is recommended, especially if it is representative of actual folding device construction. If specimens are attached to the folding test apparatus with clamps, there will be new test variables to consider, such as clamping pressure and location.

When attaching specimens to the folding apparatus using adhesive or tape, the next decision becomes where to attach the test specimen. Samples attached too close to the apex of the fold can add strain on the samples, due to lateral pulling of the samples to the mounting plates during folding. This can also add undesired variability to the test response, in addition to added strain on test specimens. Test specimen shape in the folded configuration can be measured or modeled. For our folding test method, we have defined an attachment location (denoted as  $L_{\text{free}}$  in **Figure 3b**, below) not closer than  $3 \cdot g/2$ , where  $g$  is the distance between confining test plates and attachment adhesive.

### 3.1.3 Test specimen misalignment

Misalignment of the test specimen can be caused by off-centered attachment of the test specimen, misalignment of the pivot points (non-parallel or collinear; **Figure 4**), or curved/warped mounting plates. Such forms of misalignment can result in different patterns and variability in the test response (from left to right sides of the test apparatus, for example; **Figure 5**).

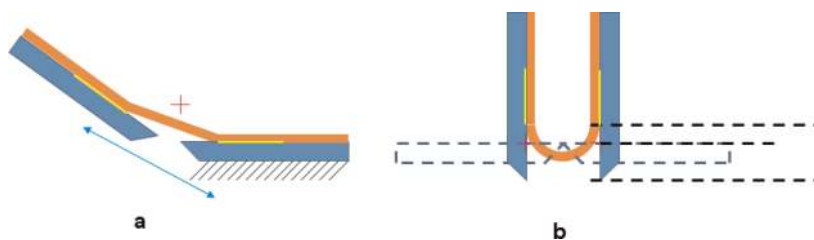


**Figure 2.** (a, b) Specimen geometry during folding for a single vs. dual pivot test apparatus. Tester mounting plates are depicted in blue, attachment adhesive is depicted in yellow, test specimen is depicted in orange, pivot locations are depicted by '+' signs. (a) shows a single pivot hinge design, in which samples can be stretched at a critical closing angle during testing. (b) shows a dual pivot hinge design, which can eliminate added stretching of the test specimen during folding. (Figures by Tom Corrigan, Ph.D. 3M Corporate Research Systems Laboratory).

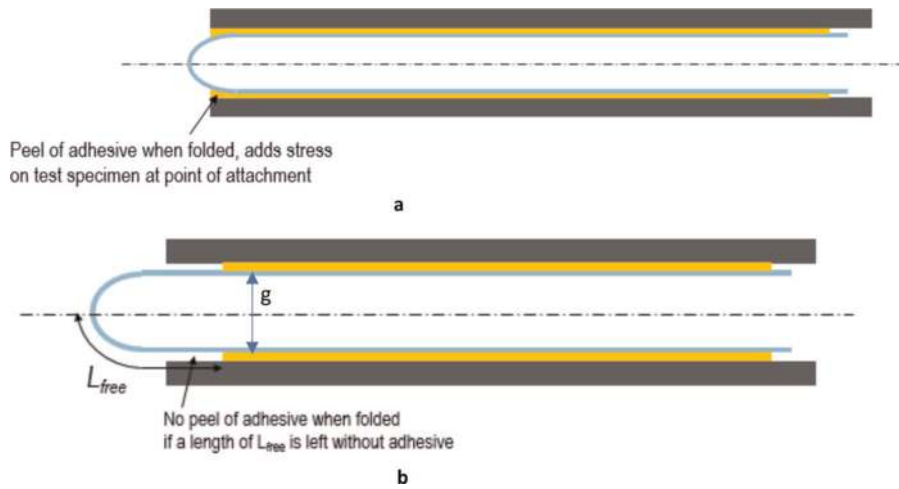


**Figure 3.** (a, b) Specimen geometry denoting location of attachment location with bond all the way to edge of substrate backing in (a), while (b) depicts a region without adhesive contact near the fold region.

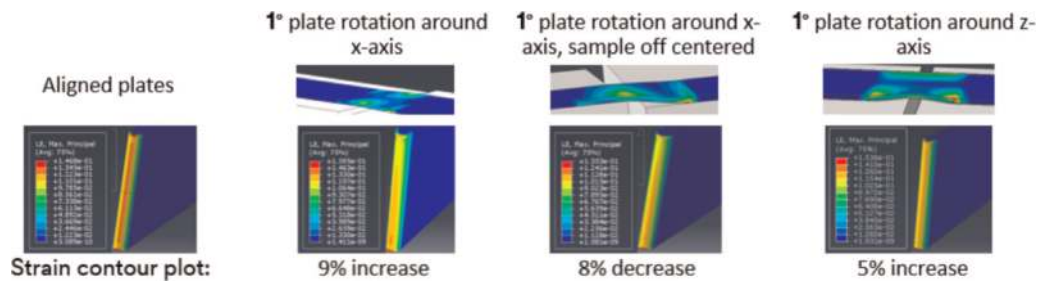


**Figure 4.** Shown above are modeling results, which depict changes in strain on test specimens depending on their alignment on the test apparatus. (Courtesy of Samad Javid, 3M Corporate Research Process Lab).

### 3.1.4 Sample conditioning and preparation

Both temperature and humidity can affect the test response, particularly for multi-layer test specimens that include adhesive in some layers, since some adhesives may be quite sensitive to moisture uptake. Dependent on the substrates used, this water uptake could apply to films, as well. Specimens should be conditioned at well-defined environmental parameters prior to testing. Testing should also take place in a controlled temperature and humidity environment. Doing so can help improve the repeatability and reliability of the test.

Lamination conditions, sample edge quality and surface treatments that impact adhesion can also influence the test response. Differing amounts of stored stress introduced during manufacturing, and tension applied during the lamination and sample preparation process can change the starting stress states of a test specimen, which can then influence the stress profiles during folding and unfolding.

### 3.1.5 Defects observed

Depicted below are several types of failure modes observed during bend testing of single and multi-layer test specimens. Crazeing (**Figure 6a**) is caused by slippage of crystal structures and void formations in polymeric films. Local buckling (**Figure 6c**) is caused by adhesion failure between layers. Global buckling (**Figure 6d**) is caused by severe instability, which can result in inverted folding of the test specimen.

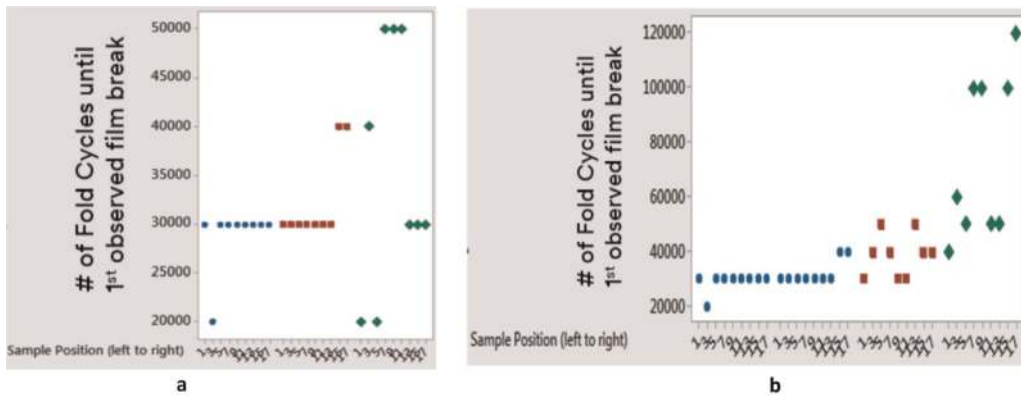


**Figure 5.**  
 (a, b) Results from testing of 4mil low melt PEN (polyethylene naphthalate) at a nominal gap size of 4 mm. Sample position is measured in inches from left to right side of test apparatus. Samples were checked every 10,000 fold cycles. (a) shows the difference in test response observed when test plates are very flat (2 test cycle replicates are depicted on this plot by red and blue), vs. curved with variation of folding gap by only 0.05 mm as measured with a feeler gauge (data depicted as a general smile pattern in green). (b) shows a sinusoidal test response (plotted in red and green) as a result of loose bearings design, which control the motion profile of the test plates. Tighter bearings design, in this case, yield a flatter more controlled test response profile (plotted in blue).

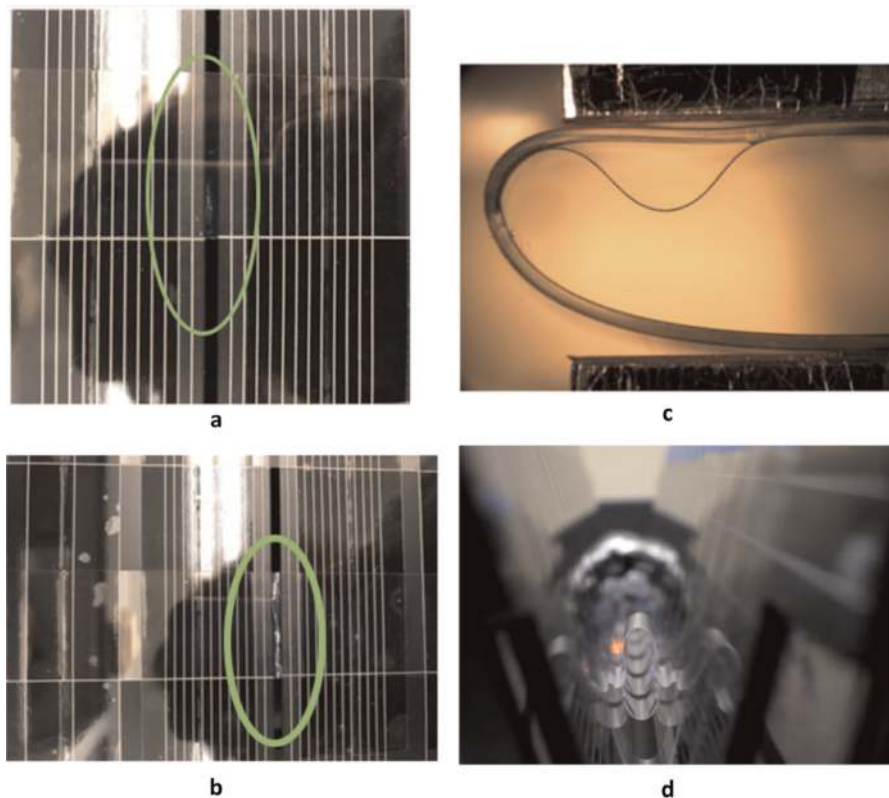
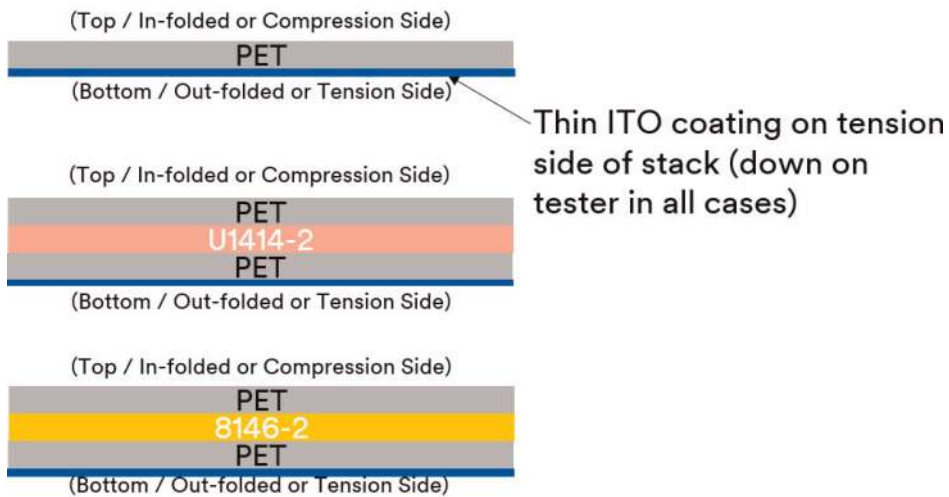


**Figure 6.**  
 Depiction of typical failure modes in foldable testing, including substrate crazing (whitening) (a), breakage (b), local buckling (c) and global buckling (d).

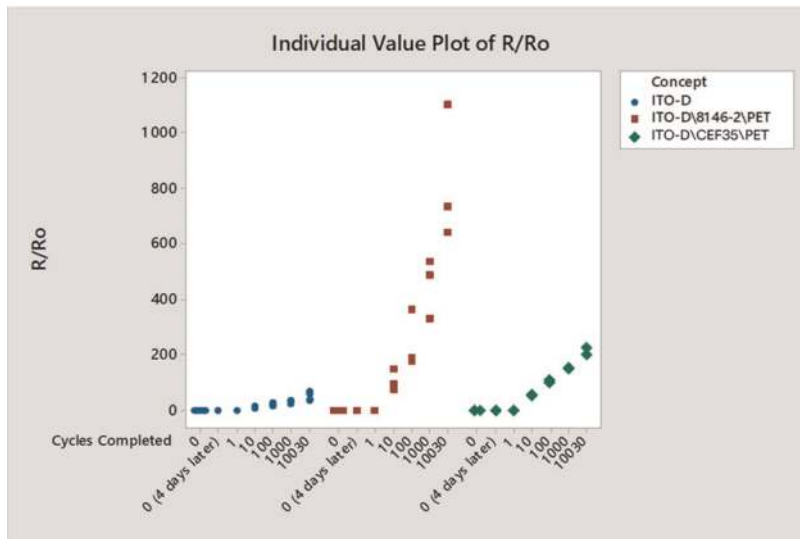
### 3.2 A test for OCA decoupling and neutral plane management

There is widely available literature to explain the effects of decoupling and isolating multiple neutral planes in a multi-layer construction [14, 29]. In the ideal

### Sample Constructions:



a



b

**Figure 7.**

(a) shows descriptions of test specimens comprising a single layer of 2mil PET, and 3-layer samples comprising of 2mil 3M<sup>®</sup> OCA 8146-2 (a standard 3M OCA) and 2mil 3M<sup>®</sup> CEF35 (a 3M foldable OCA). (b) Results show that less resistance increase is observed for the test specimens comprising of 3M<sup>®</sup> foldable OCA, CEF35, than for specimens containing standard 3M<sup>®</sup> OCA 8146-2. These results suggest that the strain amplitude on the tensioned ITO coated side of the test specimen is reduced when using 3M<sup>®</sup> foldable OCA, thus reducing damage to the fragile coating.

case, the neutral planes of each layer in the composite construction are preserved by frictionless slip (or perfect decoupling of each layer). In reality, the lay-up construction (modulus and thickness of each layer), in addition to assembly (such as tension during the lamination process) of the test specimen or display stack will influence stress profiles. 3M Foldable OCA has a lower modulus over a wide range of operating temperatures, as compared to standard commercial OCAs. This offers greater ability to decouple the stiff layers in a flexible display module and reduce the overall bending strain [29, 30].



A simple experiment was performed to assert the performance of 3M™ OCA CEF35, a 3M Foldable OCA. A thin layer of ITO was coated onto 2mil PET. The ITO coated PET was used to create 3-layer test specimens, comprising either a standard OCA 8146–2 or CEF35 at the same thickness of 2 mils (**Figure 7a**). The test specimens were folded, with ITO on the out-folded/tension side, using a dual pivot bend tester. The folding rate for this test was 30 cycles per minute, with nominal folded gap size of 4 mm. Samples were conditioned for 24 h and tested at 23C, 50%RH. Electrical resistance of the ITO coating was measured at the end locations of each test specimen (using an Ohm meter) after 0, 1, 10, 100, 1000 and 10,000 fold cycles. Results (**Figure 7b**) showed significantly less resistance increase for stacks constructed with CEF35 than for those containing OCA 8146–2, proving experimentally that CEF35 more effectively decouples the polymer film layers, due to a lower shear modulus ( $G'$ ) and higher yield under minimal load, thus, causing less damage to the conductive layer.

### 3.3 Folding test method summary

In conclusion, there are several factors to consider when designing a reliable and repeatable folding test method. Factors such as hinge or pivot design, attachment location, sample and fold axis alignment, as well as sample preparation and conditioning, and surface treatments can all have an impact on the reliability and repeatability of the test. Once these factors are controlled, the folding test can be an effective tool for use in differentiating multi-layered constructions representative of foldable displays. IEC standard 62715-6-1 [31] can be referenced and calls out several different methods of bending deformation that can be used to evaluate Flexible Display Devices. Common failure modes include crazing, breakage, local and global buckling. Most, if not all, of these failure modes can be influenced by the properties of the adhesive used to construct the test specimen. 3M Foldable OCA can help to decouple the polymeric film layers of a multi-layer test specimen, and therefor reduce strain on fragile coatings and components, due to its low modulus as compared to standard OCAs, such as 3M OCA 8146.

## 4. Modeling of foldable OLED panels

For foldable AMOLED (OLED) display panels, the repeated folding and unfolding create new mechanical requirements and challenges beyond those of fixed displays. In most applications, the multiple functional layers of a foldable display are bonded by optically clear adhesives (OCA) to form a multilayered thin panel or film stack that is flexible to allow folding of the panel.

The folding of a multilayered panel will introduce bending stress and shear stress not only within the individual layers but also between the bonded layers. Depending on the panel layout design, these bending stresses can reach very high levels causing various failures including fracture of individual layers or sensitive components within a layer, delamination, and buckling. Understanding the nature of these stresses will help in producing robust designs that ensure reliable folding performance.

Because the folding of a display by nature is a problem of large deflection of a multilayer film stack, the classical beam bending theory such as the Euler–Bernoulli approach will be limited in its ability to describe accurately the bending stress and interlaminar stress. The thin nature of the OLED display also makes it difficult to experimentally measure the stresses or visualize the deformation of the layers

within the panel. Modeling then becomes an effective tool to provide insights into the mechanical folding behavior. Numerical analysis methods, such as finite element analysis (FEA), offer detailed information of stress and related deformation in each layer of the film stack, and allow virtual testing to evaluate different design scenarios [14, 32–35].

In this chapter, we will provide an introduction of the folding simulation of OLED display panels. The aim is to demonstrate the basic process of modeling the folding and the potential failure modes of foldable displays to help design engineers to become familiar with:

- The interactions between layers of the display film stack with its bonding layers, the OCA layer, and the role of OCA on the folding performance of the film stack.
- Some basic modeling methods to simulate the folding of the film stack and the OCA.

As general guidance, we will use modeling examples of a simplified but representative display film stack to describe and discuss the models and the results.

We will also focus on the roles of the soft bonding layer, the OCAs, in the discussions of the modeling results. We will examine the overall performance of the film stack to provide basic understanding of the effectiveness of a soft bonding layer in reducing bending stress and mitigating related potential failure modes. This understanding can be valuable because the material properties and thickness of the functional layers in a display, such as the OLED, circular polarizer film, and the touch sensor film are designed to achieve their specific optical or electronic functions, and the options to vary the thickness and material properties of these functional layers may be limited. Managing a film stack's neutral plane by employing thicker or stiffer supplementary layers may be undesirable if the display panel is to be flexible. On the other hand, when the display panels become thinner, this imposes its own set of challenges in durability and usability. Optimization of the display film stack through the design of the bonding layer becomes an attractive and often a necessary option.

#### **4.1 OLED panel and construction**

The typical functional layers of an OLED film stack may include: cover film, the touch sensor layer, circular polarizer, thin film encapsulation (TFE) layer, the AMOLED (OLED) display unit, the back sheet, substrate, and others. The OLED display unit itself also consists of multiple components including a flexible substrate, encapsulation/barrier, thin film transducer (TFT), and transparent electrode. In more recent developments, display manufacturers are also pursuing integration of some of these components for thin form factors with fewer layers. The OCAs are placed between layers to bond them into an integrated display film stack that is flexible to allow folding as shown in **Figure 1**. The common industry practice for specifying the extent of the folding is by the radius of curvature of the folded region.

#### **4.2 Design requirements for foldable multilayered display panel**

The folding of a multilayered panel will introduce bending stresses, both in-plane tensile or compressive stresses and shear stresses between the layers. While each individual layer is flexible to withstand being folded into a small radius of

curvature, the bonded multilayer panel will exhibit a much higher stiffness due to the larger thickness of the whole panel, and potentially generate very high bending stresses. The high bending stresses may cause failure in various forms. Of the various components and layers in an OLED display panel, the permeation barrier layer, the indium tin oxide (ITO) layer, and the oxide dielectric layers of thin film transistors (TFT) are sensitive to tensile stress and strain, and they can fracture at a relatively low tensile strain [24, 36].

While there are many other design requirements for a display unit, in terms of folding mechanical performance, flexibility, integrity, and durability without damage are required, and fracture, delamination, or buckling under repeated bending must be prevented.

Other design requirements, including impact resistance to drop impact of display device or ball/foreign object impact, and scratch resistance are also critical for foldable displays. They are interrelated with the foldability performance, and often have competing design requirements. A more systematic and holistic design approach is necessary to incorporate all the aspects of design to achieve balanced optimal performance with some trade-offs, if necessary, among the various competing design requirements. Various modeling work has been performed in these areas at 3M, however, this belongs to a more expansive scope beyond that of the current chapter. For a more focused discussion, this modeling section will be limited to the topic of integrity for foldability.

In the following sections, the general practice of finite element analysis for simulating the folding of a film stack will be discussed first, followed by a modeling example to illustrate the potential failure modes of the film stack that need to be addressed in the design of foldable displays and the effects of OCA in mitigating these failure modes.

### **4.3 Finite element analysis of folding of display film stack**

#### *4.3.1 Finite element analysis models*

The thin film nature of the film stack makes it suitable for using a 2D model to represent the stack without losing much fidelity, especially when edge effects are not significant. To model the interactions among the different functional layers, each layer should be modeled as an individual part of the film stack. In particular, this simulates the deformation behavior that is critical in understanding the effects of OCA on the folding performance of film stack. The finite element mesh size should be sufficiently fine to resolve the stress gradient of the critical layers both in their thickness direction and in the in-plane direction, especially in the bend region where stresses vary through the thickness direction.

The bonding of the OCA to film can be simulated by various interaction definitions such as nodal constraint or node coupling of the mesh of the OCA layer to the mesh of the substrate film layer. This approach will typically not allow the simulation of the separation or debonding of the OCA from the substrates, however, it can offer most of the needed information to evaluate the bond performance without the added complexity of simulating the debonding process. To simulate the debonding process, cohesive elements may be used to represent the OCA bond. If cohesive elements are used, care should be taken to incorporate the cohesive law that describes the debonding force-displacement of the OCA bond attached to the specific films of the actual application because the bond strength depends on the specific substrate films. Also, separate cohesive laws for tension (normal to bond interface) and shear should be used to accurately represent the OCA bond behavior which will require calibrations of the cohesive laws from test data such as those

from butt joint or T-joint tests and lap shear tests. In general, the correct application of cohesive elements or cohesive contact for OCAs is more involved. Proper training on the technique will help to avoid misrepresentation of OCA bonds. It is recommended that users consult with 3M technical support for test methods or test data related to bond strength simulation.

#### *4.3.2 Modeling OCAs*

Being a type of pressure sensitive adhesive, OCA needs to be soft enough to flow under application of pressure to wet the substrate in close proximity. This intimate contact between OCA and the substrate allows molecular interactions such as van der Waals forces to form the basis of the adhesion that underwrites the overall bond strength. This flow-like behavior of OCA can be described by a combination of nonlinear elastic and viscoelastic/viscoplastic material models.

For OCA's viscoelastic behavior, its relaxation function can be defined in terms of a series of exponentials known as the Prony series. For the nonlinear elastic or hyperelastic constitutive models, the models such as the polynomial hyperelastic models are most commonly used. They include the neo-Hookean model, Mooney-Rivlin model, and Yeoh model. All are effective in describing OCAs' ability to be stretched to very large strain. Other forms of hyperelastic models including Arruda-Boyce and Ogden models may also be used. The commercial finite element analysis packages, such as ABAQUS, ANSYS, and COMSOL offer the finite strain computational methods and material model libraries that allow advanced simulation of OCAs. Users can apply the material model calibration tools provided by the finite element analysis software packages to evaluate the material parameters for these constitutive models from OCA material characterization test data. It is also recommended that they contact 3M technical support for information on OCA material data for their specific applications.

#### *4.3.3 Material characterization tests*

Several material characterization tests are needed to generate data for the calibration of the constitutive models mentioned above. For calibrating the elastic or hyperelastic material models, one or more of the tests listed below needs to be performed on the OCA:

- Uniaxial tensile
- Simple shear
- Biaxial tensile
- Compression and/or bulk compression

For viscoelastic model calibration, the dynamic mechanical analysis (DMA) test can be performed to produce master curves of the storage modulus and loss modulus of OCA to calibrate the Prony series. Otherwise, relaxation or creep test data at various strain rates and temperatures of interest may be used for the Prony series calibration.

For calibration of OCA bond strength models, such as the cohesive zone model, the proper measurements of the bond strength using T-joint specimens and lap shear specimens should be emphasized. These tests should be performed on the actual substrate materials of the film stack, especially if the potential failure mode



may be adhesion failure. 3M Technical Support can be a source for information related to the test methods for adhesive characterization.

#### 4.4 Examples of finite element analysis of folding performance of a foldable display film stack

The following is an example of finite element analysis of dynamic folding simulation of a display film stack, followed by discussions of the analysis results to assess the folding performance.

In the finite element analysis (FEA) presented here, a simplified 7-layer film stack was used to represent a foldable OLED display (**Table 2**). The film stack was assumed to be attached to two rigid back plates joined by hinges. The center portion of the film stack was not attached to the rigid back plate to allow for folding of the stack. The folding action simulated here is the so-called ‘out-folding’ such that the film stack is folded towards its back layer. In the fully folded configuration, the space between the straight sections of the outer layer is 10 mm resulting in the bend section of the film stack forming an approximate semi-circle of radius 5 mm as shown in **Figure 8**. In the simulation, the film stack was folded in 3 s, then held in the folded configuration for 24 h before it was unfolded in 3 s. The material properties and the thickness of each layer used in this work are listed in **Table 2**. The total thickness of the film stack simulated here was 0.475 mm (layout 1) and 0.275 mm (layout 2). The simulation was repeated for the two film stack layouts bonded by 3M™ Foldable OCA CEF35 and 3M™ OCA 8211. 3M™ CEF35 has a lower storage modulus than that of 3M™ OCA 8211, and exhibits a more elastic behavior as indicated by its lower Tan delta value (**Table 2**) than that of 3M™ OCA 8211.

The simulation was performed using the ABAQUS finite element analysis package. Due to the large ratio of film stack panel width to thickness, a 2-dimensional

Layers	Thickness (µm)	Material	Modulus of elasticity, E, (GPa)	Storage Modulus, G', (GPa) at frequency of 1 rad/s	Tan Delta
Cover film	150 (50)	PET	3.5	NA*	NA
OCA	25	3M™ CEF35 (OCA 1) 3M™ OCA 8211 (OCA 2)	/	0.03E-3 0.07E-3	0.33 0.70
Circular polarizer	75 (125)	Triacetate	3.2	NA	NA
OCA	25	3M™ CEF35 (OCA 1) 3M OCA 8211 (OCA 2)	/	0.03E-3 0.07E-3	0.33 0.70
AMOLED	75	Polyimide substrate	3.5	NA	NA
OCA	25	3M™ CEF35 (OCA 1) 3M OCA 8211 (OCA 2)	/	0.03E-3 0.07E-3	0.33 0.70
Back plate	100 (150)	PET	2.7	NA	NA

\*NA = Not Applicable

The thickness shown in brackets in the table are the values used for stack layout 2.

**Table 2.**

The simplified 7-layer display film stack layout and the properties used in the simulation.

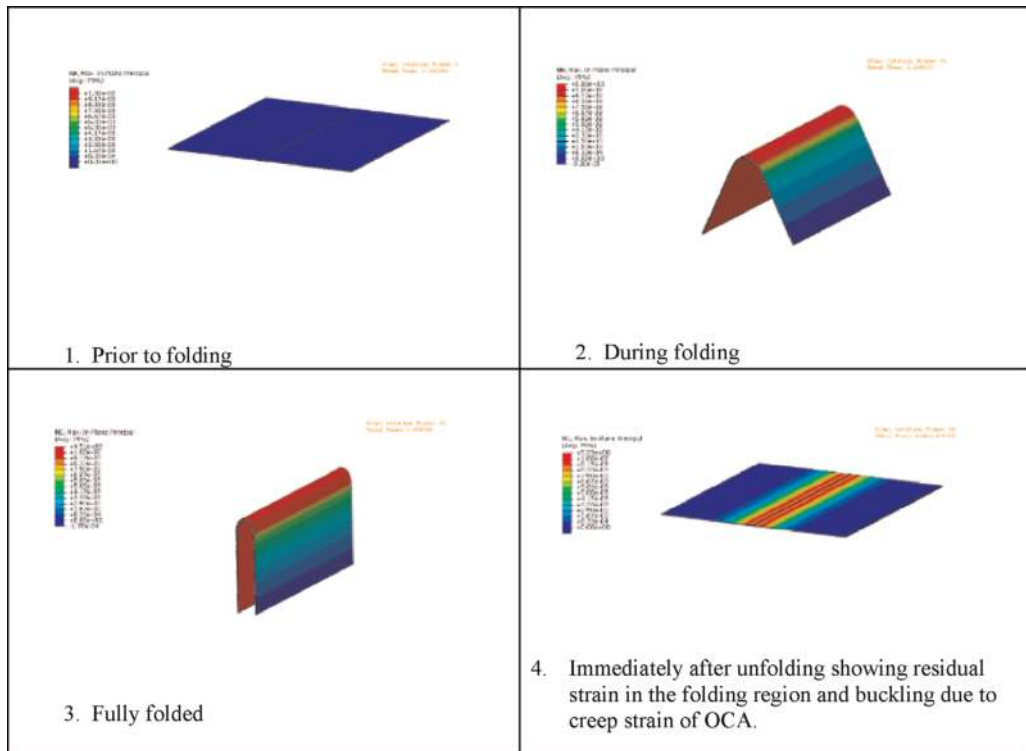


**Figure 8.** Simulation results showing the 4 stages of folding. The film stack is folded towards its back layer in the form of the so-called “out-folding”.

plane strain model meshed with the plane strain solid element, CPE4, was used. Six elements were used through the thickness for the OCA layer, and four elements through the thickness for each of the other functional layers.

#### 4.4.1 Discussions of the simulation results

The following potential failure modes typical for foldable displays were predicted for various film stack layouts by the simulation and are also observed in experiments:

- Failure due to tensile strain from bending exceeding the critical values for specific components/layers in the display film stack
- Buckling
- Debonding between layers of the film stack

**Figure 9** shows the finite element analysis results of these failure modes. In the following sections, each will be discussed with emphasis on the effects of OCA’s soft properties on the bending performance.

#### 4.4.2 Fracture and failure due to tensile strain, multiple neutral planes due to large shear strain of OCA

For film stacks bonded by 3M™ CEF35 and 3M™ OCA 8211, the results show that the lower modulus of 3M™ CEF35 allows large shear slippage between layers leading to reduced bending stress in the film stack. The in-plane strain in the OLED

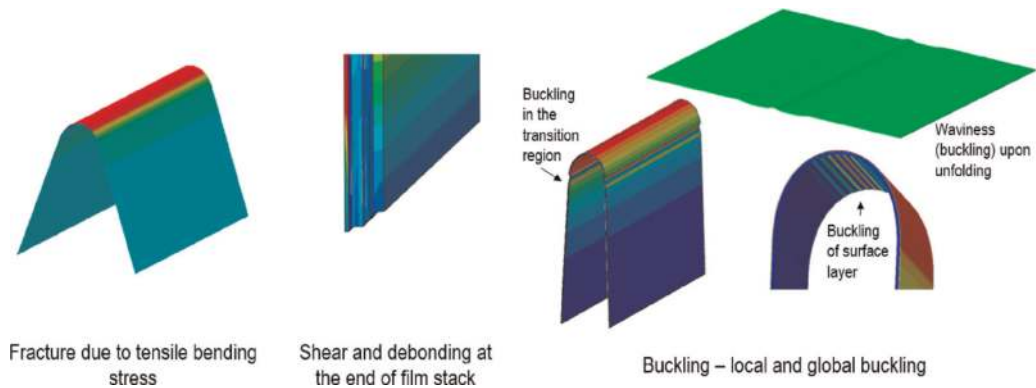


**Figure 9.**  
 The predicted potential failure modes of foldable display film stack.

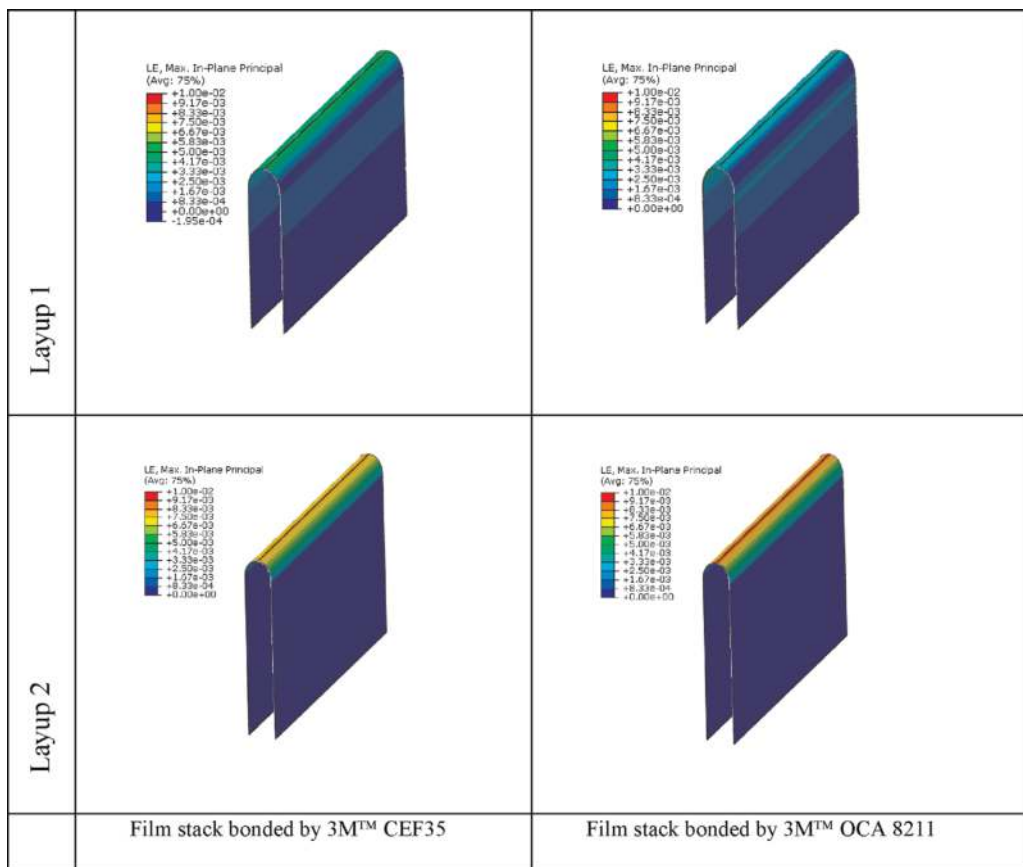


**Figure 10.**  
 Contour plots of in-plane bending strain in the OLED layer when the film stack is fully folded for the film stacks bonded by 3M OCAs (only the OLED layer is shown in this figure).

layer is shown in **Figure 10** for the two film stacks bonded by 3M™ CEF35 and 3M™ OCA8211. The maximum tensile strain occurs in the bend section at the bending symmetry plane after the film stack is completely folded. The maximum tensile strain ranged from 0.2% to 0.6% in the stacks bonded by 3M™ CEF35, and from 0.4% to 0.9% for stacks bonded by 3M™ OCA 8211. Depending on the critical strains of the OLED, ITO, or TFE, a less stiff OCA may make the difference between failure and no-failure of the display panel.

When the OCA's shear deformation between layers is sufficiently high to allow adjacent layers to slip over each other, each layer can bend without much constraint from the adjacent layers. This shear decoupling effect can result in much reduced bending stresses in some of the layers leading to a neutral plane in each of the layers, especially for the layers closer to the center of the film stack. In **Figure 11**, the bending stress (the stress in the direction parallel to the neutral plane of the film stack) of the film stack bonded by 3M™ CEF35 is shown. The plot shows the bending stress distribution at the cross-section of A-B, which is the location where the maximum bending stress will occur within the bend region of the film stack. For this 7-layer film stack of a total thickness of 0.475 mm (**Table 2**), the bending stress on each of the three OCA layers is negligible due to its low stiffness. The low stiffness of OCA, on the other hand, facilitates relatively high shear strain, in the range of 300–400% (**Figure 12**). This large shear strain between the layers allows each of the CWF, OLED, and back plate films to bend relatively independently from others resulting in a neutral plane in each of these functional layers, as indicated by the zero-bending stress location within each layer.

The ability of soft OCA to shear easily provides an effective design option to achieve multiple neutral planes in a film stack. This can be of great value since it can enable more freedom of choice regarding material properties and thicknesses of other functional layers without compromising their specific optical or electronic performance in a display.

#### 4.4.3 Buckling

Under bending, a thin display film stack that is partially attached to a stiffer back plate is susceptible to buckling failure that leads to optical distortion and possible debonding, either within the film stack layers or from the back plates on which the

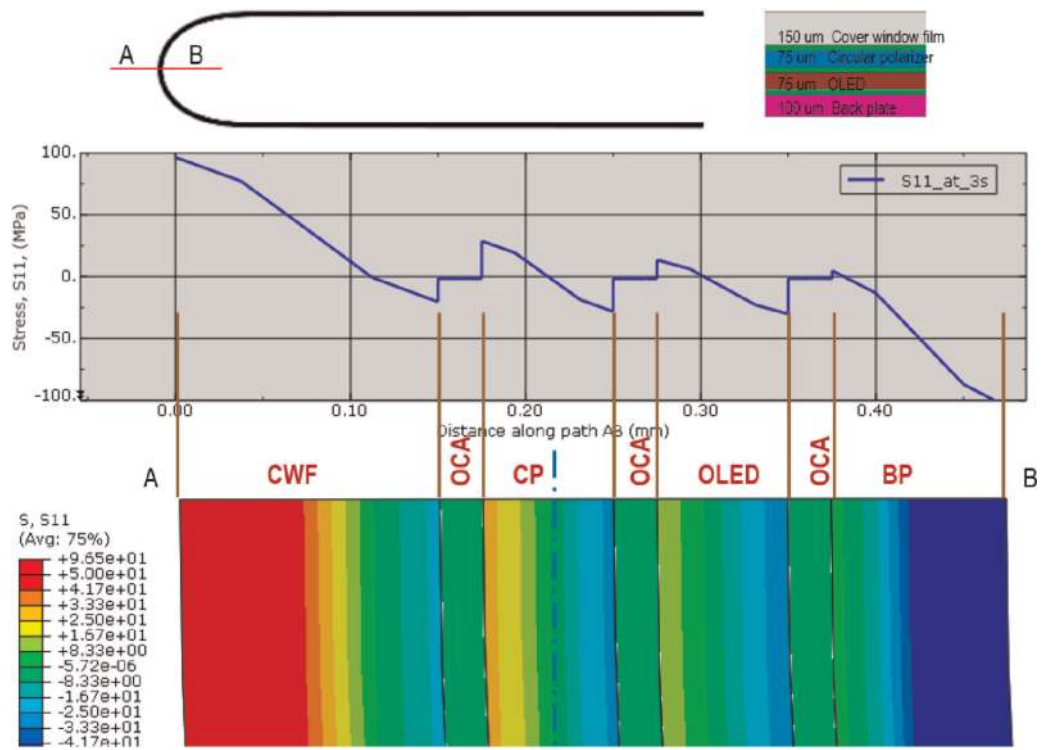


**Figure 11.** Bending stress distribution at the cross-section A-B which is the plane of symmetry of the folded film stack.



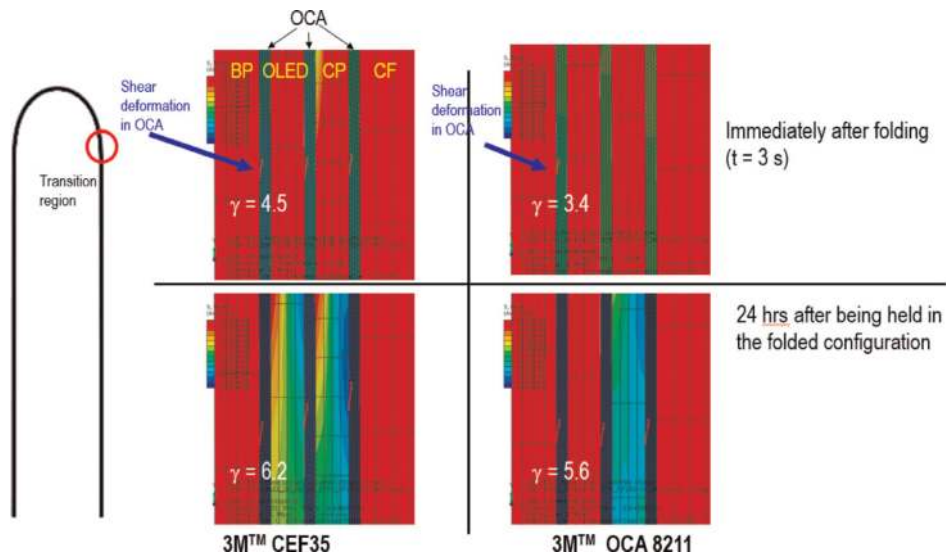


**Figure 12.** Contour plots of shear stress in the transition region for the film stack (layout 1) showing the large shear deformation of the OCA layers.

film stack is attached. Buckling of the film stack can be further categorized into global buckling and local buckling types.

Global buckling typically gives the film stack a wavy appearance. It happens during unfolding after the film stack is held in the folded configuration for a period of time. In the folded configuration, shear creep in the OCA may occur which can be observed at the end of the film stack where each layer slips over the adjacent layer (**Figure 13**). This creep induced shear slip cannot be immediately recovered upon unfolding. During unfolding, the top layers of the film stack shown in **Figure 11** will then be under compression while the bottom layers will be in tension. Depending on the amount of the shear creep and the overall stiffness and thickness of the film stack, this may lead to instability and global buckling as shown in **Figure 14**. The more elastic behavior of 3M™ CEF35 limits the shear creep deformation and, in turn, leads to reduced buckling during unfolding.

Local buckling often appears as a fine and thin wrinkle or wrinkles on the surface on the compressive side of the folded film stack [36]. It occurs during folding but may still be visible after unfolding if the buckling is allowed to set in over a period of time or if the buckling causes debonding in the region.

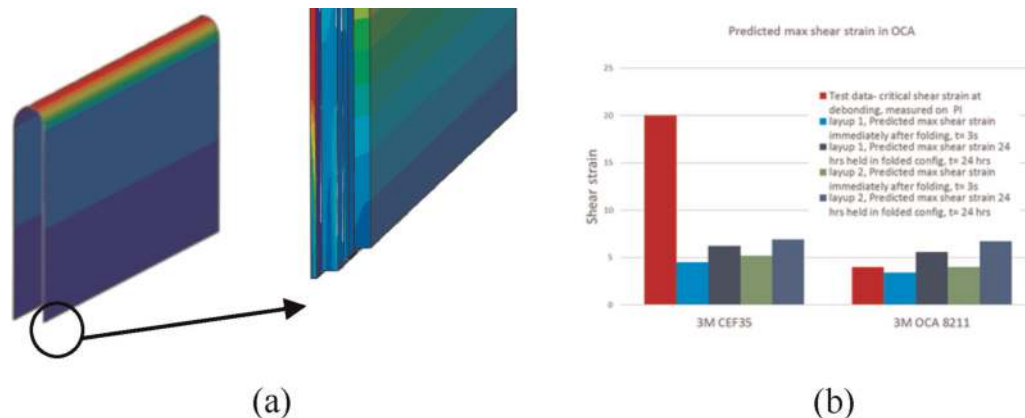


**Figure 13.** Simulation results showing the shear deformation between layers (a), and the predicted maximum shear strain in OCA layer and the comparison with the bond strength of the OCA (b).

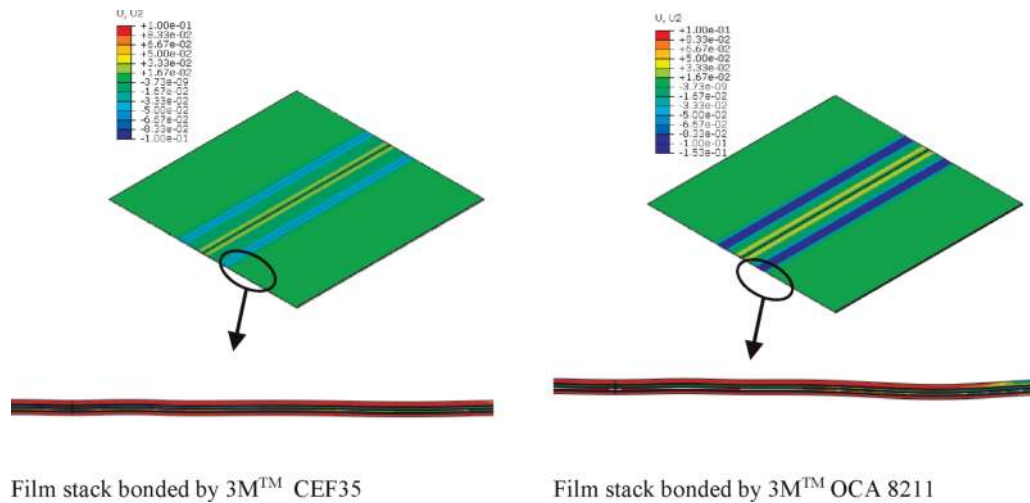


**Figure 14.** Displacement contour plots comparison of buckling of the film stack bonded by 3M™ CEF35 and 3M™ OCA 8211 immediately after unfolding showing the improved buckling resistance of 3M foldable OCA. The displacement,  $U_2$ , is in the direction perpendicular to the film surface (unit: mm).

During folding, high compressive stress can develop in the bend region. Local buckling occurs only in the layers on or close to the surface of the film stack on the compressive side of the neutral plane. If the compressive stresses in these layers are not reduced through OCA's shear deformation, they may cause these layers to buckle or bulge out especially if any geometric off-axis imperfection is present in these layers. As shown in **Figure 15**, the buckling deformation will stretch the OCA that bonds the buckled layers to the remaining un-buckled layers resulting in tensile stress in OCA in the direction perpendicular to the bonding interface. Depending on the OCA bond strength, this tensile stress can cause delamination in this region.

Local buckling was not predicted in the film stacks bonded by 3M™ CEF35 or 3M™ OCA 8211 (the layup specified in **Table 2**). However, if the OCA modulus is reduced to 10% of that of 3M™ CEF35, the simulation predicted that local buckling could occur which is shown in **Figure 15** for a particular film stack. On the other hand, reducing the thickness of OCA to increase the constraint to buckling deformation can effectively improve the local buckling resistance as shown in **Figure 16**. Our studies have shown that reducing OCA thickness and increasing OCA stiffness can improve film stack's buckling resistance, while reducing OCA stiffness



**Figure 15.** Predicted local buckling on a film stack bonded with an OCA with a stiffness of 10% of that of 3M™ CEF35. The inserts are the photos of a local buckling on the actual film stack.

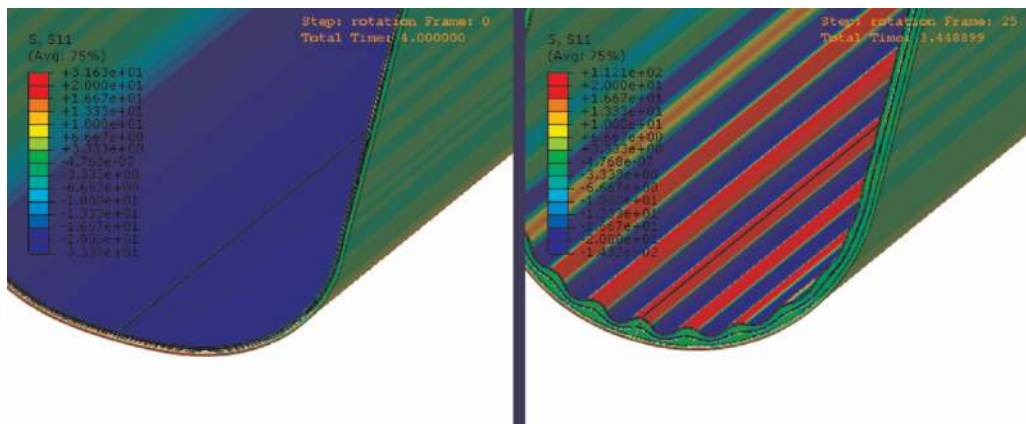


**Figure 16.** Simulation results showing the effect of OCA thickness on local buckling. The film stacks shown here were bonded with 3M OCA of different thickness. The ratios of the surface layer thickness to the underlying OCA layer thickness is 2.0 for the layup on the left, and 1.0 for the layup on the right.

to facilitate shear slip is also critical in reducing the compressive stress that is the root cause of buckling. All these demonstrate that the design for buckling resistance is a balancing act and represents one of the most challenging aspects in film stack optimization. The competing requirements of stiffness to resist buckling and flexibility for folding, as well as, for minimizing the cause of buckling further highlights the importance of leveraging OCA's broader range of properties to achieve the optimal film stack performance.

#### 4.4.4 Delamination and debonding

Another failure mode often observed in the foldable display is delamination or debonding, which is characterized by separation of layers either near the ends of the display panel, or within the bend region.

Typically, the debonding at the end of the film stack is due to shear strain in the OCA exceeding the OCA bond shear strength, while the delamination within the bend region is the result of high interlayer tensile stresses on OCA due to local buckling as described above.

In **Figure 12**, the shear stress of the film stack is shown for the transition region where the bent section meets the straight section. The corresponding shear strain values are indicated on the plots. **Figure 13** shows the shear stress at the end of the film stack. For both the film stacks bonded by 3M™ CEF35 and 3M™ OCA 8211, along the length of the film stack, the maximum shear strain occurs in the transition region. The higher the shear strain in the OCA, the more shear slip is allowed between layers, which reduces the bending stress in the layers. For the layers on the compressive side of the neutral plane, this means reduced compressive stress and the reduced possibility of local buckling of these layers. For the layups simulated in this work, the shear strain can be as high as 600% as shown in **Figure 12**. The softer 3M™ CEF35 allows not only large shear strain upon folding leading to improved local buckling resistance, it also can effectively resist debonding due to its high bond strength (**Figure 13**).

## 5. Summary

The simulation examples of folding OLED display film stacks discussed here demonstrate OCAs' abilities to reduce bending stresses and to create multiple

neutral planes in a film stack. The simulation examples also demonstrate three potential failure modes for film stacks under dynamic folding and unfolding.

- Fracture due to high tensile bending stress
- Buckling
  - Local buckling of a few layers in the film stack and global buckling of the panel where the entire film stack buckles and assumes a wavy form
- Delamination or debonding

As shown in these simulation examples, these failures can be addressed through design and selection of appropriate OCAs. It is also evident that the folding performance of a display is a system-level response, where performance is governed by the properties of each layer in the stack layout as well as the display attachment methods and folding hinge design. The softest layers in the film stack, the OCAs, play a critical role in optimizing the film stack's folding performance when the options to alter the mechanical properties or thickness of other functional layers to improve overall stack flexibility are restricted by their designed functionalities. Design of display film stacks that utilize OCAs' unique characteristics can lead to increased robustness of integrated system solutions for foldable displays.

### **Conflict of interest**

The authors declare no conflicts of interest.

### **Author details**

Joel T. Abrahamson<sup>1</sup>, Hollis Z. Beagi<sup>1</sup>, Fay Salmon<sup>2</sup> and Christopher J. Campbell<sup>1\*</sup>


<sup>1</sup> 3M Display Materials and Systems Division, Saint Paul, Minnesota, United States

<sup>2</sup> 3M Corporate Research Systems Lab, Saint Paul, Minnesota, United States

\*Address all correspondence to: [cjcampbell@mmm.com](mailto:cjcampbell@mmm.com)

### **IntechOpen**

---

© 2019 The Author(s). Licensee IntechOpen. This chapter is distributed under the terms of the Creative Commons Attribution License (<http://creativecommons.org/licenses/by/3.0>), which permits unrestricted use, distribution, and reproduction in any medium, provided the original work is properly cited. 

## References

- [1] Which was the first mobile phone to market with a capacitive touchscreen? [Internet]. 2018. Available from: <https://www.techspot.com/trivia/11-what-first-mobile-phone-market-capacitive-touchscreen/> [Accessed: 16 December 2018]
- [2] Samsung Galaxy Round: The World's First Curved OLED Phone [Internet]. 2018. Available from: <https://www.ign.com/articles/2013/10/09/samsung-galaxy-round-the-worlds-first-curved-oled-phone> [Accessed: 16 December 2018]
- [3] Samsung Galaxy Note Edge [Internet]. 2018. Available from: [https://www.gsmarena.com/samsung\\_galaxy\\_note\\_edge-6631.php](https://www.gsmarena.com/samsung_galaxy_note_edge-6631.php) [Accessed: 16 December 2018]
- [4] Israelachvili J. *Intramolecular & Surface Forces*. 3rd ed. London: Academic Press; 2011. 450 p. DOI: 10.1016/c2011-0-05119-0
- [5] Pocius A. *Adhesion and Adhesives Technology*. 3rd ed. Carl Hanser: Munich; 2012. 386 p. DOI: 10.3139/9783446431775
- [6] Kinloch A. *Adhesion and Adhesives*. Vol. 441p. London: Chapman and Hall; 1987. DOI: 10.1007/978-94-015-7764-9
- [7] Dahlquist C. Tack. In: *Adhesion: Fundamentals and Practice – A Report on an International Conference Held at the University of Nottingham, England; 20–22 September 1966; Nottingham*. London: Ministry of Technology; 1969. p. 143
- [8] Lakrout H, Sergot P, Creton C. Direct observation and fibrillation in a probe tack experiment on model acrylic pressure-sensitive-adhesives. *The Journal of Adhesion*. 1999; **69**:307-359. DOI: 10.1080/00218469908017233
- [9] Campbell C. Optically clear adhesives. In: Chen J, Cranton W, Fihn M, editors. *Handbook of Visual Display Technology*. 2nd ed. Berlin: Springer; 2016. pp. 1501-1514. DOI: 10.1007/978-3-319-14346-0
- [10] Everaerts A, Xia J. Cloud point-resistant adhesives and laminates. US Patent 8,361,632; 2013
- [11] No DH, Kim JW, Kamine T, Hwang HD. Display Device Comprising Polarizing Layer. US Patent Application 20160093833; 2016
- [12] Cho HS, Jin C, Kim EH, Yoo SH. Polarizer-free, high-contrast ratio organic light-emitting diodes utilizing microcavity structures and neutral-density filters. *Journal of Information Display*. 2014; **15**:195-199. DOI: 10.1080/15980316.2014.970238
- [13] Gower M, Shanks R. Acrylic acid level and adhesive performance and peel master-curves of acrylic pressure-sensitive adhesives. *Journal of Polymer Science Part B Polymer Physics*. 2006; **44**:1237-1252. DOI: 10.1002/polb.20779
- [14] Salmon F, Everaerts A, Campbell C, Pennington B, Erdogan-Haug B, Caldwell G. Modeling the mechanical performance of a foldable display panel bonded by 3M optically clear adhesives. *SID Digest*. 2017; **48**(1):938-941. DOI: 10.1002/sdtp.11796
- [15] Royole Introduces 'FlexPai', the World's First Commercial Foldable Smartphone With a Fully Flexible Display, A Combination of Mobile Phone and Tablet [Internet]. 2018. Available from: <https://www.royole.com/Dynamics?id=578> [Accessed: 08 January 2019]
- [16] Galaxy Fold [Internet]. 2019. Available from: <https://www.samsungmobilepress.com/galaxy-fold> [Accessed: 20 March 2019]



- [17] HUAWEI Mate X, 5G Smartphone, Foldable Design [Internet]. 2019. Available from: <https://consumer.huawei.com/en/phones/mate-x/> [Accessed: 20 March 2019]
- [18] LG OLED65R9PUA 65 Inch Class LG SIGNATURE OLED TV R9 [Internet] 2019. Available from: <https://www.lg.com/us/tvs/lg-OLED65R9PUA-signature-oled-4k-tv> [Accessed: 20 March 2019]
- [19] Sun Z, Meng C, Ho J, Tseng K, Kwok H. Fabrication of broadband quarter wave plate by combination of two retardation films using coating technique. *SID Symposium Digest of Technical Papers*. 2018;**49**:222-224. DOI: 10.1002/sdtp.12687
- [20] Zhou Y, Zhao Y, Reed JM, Gomez PM, Zou S. Efficient circular polarizer using a two-layer nanoparticle dimer array with designed chirality. *Journal of Physical Chemistry C*. 2018; **122**:12428-12433. DOI: 10.1021/acs.jpcc.8b02113
- [21] Ma X-L, Chen X-C, Xiao L, Wang H-Y, Tan J-F, Song P, et al. P-126: A New Coatable Circular Polarizer for Anti-Reflection of Flexible AMOLED, *SID Symposium Digest of Technical Papers*, 2017; 48. DOI: 10.1002/sdtp.11998
- [22] Liu Z, Mao X, Wang, M-HSI, Gu X, Shi S-m, Zhou W-F, et al. A Stack of Bendable Touch Sensor with Silver Nanowire for Flexible AMOLED Display Panel, *SID Symposium Digest of Technical Papers*, 2017; 48. DOI: 10.1002/sdtp.11788
- [23] Fried A, Zhang XH, Abrahamson JT, Wang C, Luo J, Monson RJ, et al. Latest advances in silver nanowire based touch module reliability. In: 2015 IEEE 15th International Conference on Nanotechnology (IEEE-NANO). Rome; 2015. DOI: 10.1109/NANO.2015.7388838
- [24] Letterier Y, Pinyol A, Gillieron D, Manson J-AE, Timmermans PHM, Bouten PCP, et al. Mechanical failure analysis of thin film transistor devices on steel and polyimide substrates for flexible display applications. *Engineering Fracture Mechanics*. 2010; **77**:660-670. DOI: 10.1016/j.engfracmech.2009.12.016
- [25] Seo S-W, Jung E, Chae H, Seo SJ, Chung HK, Cho SM. Bending properties of organic-inorganic multilayer moisture barriers. *Thin Solid Films*. 2014;**550**:742-746
- [26] Kim S, Kwon H-J, Lee HH, Shim H, Chun Y, Choi W, et al. Low-power flexible organic light-emitting diode display device. *Advanced Materials*. 2011;**23**:3511
- [27] Jimbo Y, Tamatsukuri Y, Ito M, Yokoyama K, Hirakata Y, Yamazaki S. Reliability and mechanical durability tests of flexible OLED with ALD coating. *Journal of the Society for Information Display*. 2015;**23**:313
- [28] Lee JH, Park JW, Lee TH, Shim GS, Kim HJ, Jung SY, et al. Variation of adhesion properties with molecular weight of cured and non-cured acrylic PSAs. In: *Proceedings of the 39th Annual Meeting of the Adhesion Society*. Vol. 151. 2016
- [29] Beagi H, Corrigan T, Leatherdale C, Salmon F, Javid S, Harein M, et al. Folding test method development and differentiation of multi-layer concepts containing optically clear adhesive. In: *Proceedings of the Adhesion Society*; 25 February – 1 March 2018. San Diego; 2018
- [30] Campbell CJ, Clapper J, Behling RE, Erdogan-Haug B, Beagi HZ, Abrahamson JT, et al. P-198: Optically clear adhesives enabling foldable and flexible OLED displays. In: *Society for Information Display International Symposium Digest of Technical Papers*.

Los Angeles; 2017. DOI: 10.1002/  
sdtf.12071

[31] International Electrotechnical  
Commission, IEC62715–6-2:2017

[32] Chiang CJ, Winscom C, Bull S,  
Monkmana A. Mechanical modeling of  
flexible OLED devices. *Organic  
Electronics*. 2009;**10**:1268-1274. DOI:  
10.1016/j.orgel.2009.07.003

[33] Lee CC. Modeling and validation of  
mechanical stress in indium tin oxide  
layer integrated in highly flexible  
stacked thin films. *Thin Solid Films*.  
2013;**544**:443-447. DOI: 10.1016/j.  
tsf.2013.02.084

[34] Jia YZ, Liu ZZ, Wu D, Chen JF,  
Meng H. Mechanical simulation of  
foldable AMOLED panel with a module  
structure. *Organic Electronics*. 2019;**65**:  
185-192. DOI: 10.1016/j.orgel.2018.  
11.026

[35] Liu ZZ. Stress simulation of foldable  
OLED screen bending. *Chinese Journal  
of Liquid Crystals and Displays*. 2018;  
**33**(7):555-560. DOI: 10.3788/  
YJYXS20183307.0555

[36] Leterrier Y, Me'dico L, Demarco F,  
Manson J-AE, Betz U, Escola MF, et al.  
Mechanical integrity of transparent  
conductive oxide films for flexible  
polymer-based displays. *Thin Solid  
Films*. 2004;**460**:156-166. DOI: 10.1016/  
j.tsf.2004.01.052